

The RNA-binding Motif Protein 15B (RBM15B/OTT3) Acts as Cofactor of the Nuclear Export Receptor NXF1*[§]

Received for publication, February 17, 2009, and in revised form, July 7, 2009. Published, JBC Papers in Press, July 8, 2009, DOI 10.1074/jbc.M109.040113

Hiroaki Uranishi[‡], Andrei S. Zolotukhin[§], Susan Lindtner[‡], Soren Warming^{¶1}, Gen-Mu Zhang[§], Jenifer Bear[§], Neal G. Copeland^{¶2}, Nancy A. Jenkins^{¶2}, George N. Pavlakis[‡], and Barbara K. Felber^{§3}

From the [‡]Human Retrovirus Section, the [§]Human Retrovirus Pathogenesis Section, Vaccine Branch, and the [¶]Mouse Cancer Genetics Program, Center for Cancer Research, NCI, National Institutes of Health, Frederick, Maryland 21702-1201

The human SPEN family proteins SHARP, RBM15/OTT1, and RBM15B/OTT3 share the structural domain architecture but show distinct functional properties. Here, we examined the function of OTT3 and compared it with its paralogues RBM15 and SHARP. We found that OTT3, like RBM15, has post-transcriptional regulatory activity, whereas SHARP does not, supporting a divergent role of RBM15 and OTT3. OTT3 shares with RBM15 the association with the splicing factor compartment and the nuclear envelope as well as the binding to mRNA export factors NXF1 and Aly/REF. Mutational analysis revealed direct interaction of OTT3 and RBM15 with NXF1 via their C-terminal regions. Biochemical and subcellular localization studies showed that OTT3 and RBM15 also interact with each other *in vivo*, further supporting a shared function. Genetic knockdown of RBM15 in mouse is embryonically lethal, indicating that OTT3 cannot compensate for the RBM15 loss, which supports the notion that these proteins, in addition to sharing similar activities, likely have distinct biological roles.

The SPEN (split end) family proteins share a domain architecture comprising of three N-terminal RNA-binding domains (RRMs)⁴ and a Spen paralogue and orthologue C-terminal (SPOC) domain (1–3). SPEN homologues are found from *Caenorhabditis elegans* to humans, and each species encodes one large (~3000–5000 aa) and one or two small (~500–1000 aa) proteins (see also Fig. 1). In humans, the SPEN family consists of the large protein SHARP (SMRT/HDAC1-associated repressor protein) and two small proteins, RBM15 (also referred to as OTT1) and OTT3 (also referred to as RBM15B) (see Fig. 1A). The SPOC domain present in the orthologous SPEN (*Drosoph-*

ila melanogaster), SHARP (human), and Mint (mouse) proteins interacts with SMRT/NCoR corepressor and mediates transcriptional regulation, and these proteins act as transcriptional effectors of Wingless as well as Notch signaling pathways (4–10). Human SHARP also binds to the steroid receptor RNA coactivator noncoding RNA via its RRM domains and suppresses steroid receptor transcription activity (10). Although the conserved role of the large SPEN proteins as transcriptional effectors downstream signal transduction is well established, the roles of the small proteins are less clear. Chromosomal translocations in a case of acute megakaryocytic leukemia created a fusion of the nearly full-length RBM15 with megakaryocytic acute leukemia/megakaryoblastic leukemia-1 (11, 12) that was proposed to act via the megakaryocytic acute leukemia moiety to activate transcription of serum response factor-regulated genes (13). In *Drosophila*, the large (SPEN) and small (NITO) factors can act redundantly in Wingless signaling (14) or antagonistically in eye development, via receptor tyrosine kinase signaling pathway (15), whereas the human RBM15, like its large paralogue SHARP, was implicated in Notch signaling (12), suggesting overlapping functions of the large and small proteins in these species. However, in mouse, both the large Mint protein and RBM15 are essential (Refs. 4 and 16–18 and this report), pointing to nonredundant roles. Moreover, despite the structural conservation of the SPOC domain in human RBM15, OTT3, and SHARP, only the SHARP SPOC domain is active in transcriptional regulation (19), strongly suggesting a diversified role for this domain in small proteins. Recent studies indicated that, besides their possible roles at the level of transcription, the small human proteins OTT3 and RBM15 are involved in post-transcriptional regulation (19, 20). Both proteins are localized to the nucleus and do not shuttle to the cytoplasm (19, 20), suggesting participation in nuclear events. OTT3 was identified as an interaction partner of the Epstein-Barr virus mRNA export factor EB2 and was shown to act as an mRNA splicing regulator (19). RBM15 was shown to bind to the RNA transport element RTE (20). RTE is found in mouse intracisternal A particle retroelements (21, 23, 34) and is essential for intracisternal A particle mobility (21). RTE is also able to replace the Rev-RRE regulation in HIV-1, demonstrating its potency as RNA export element (23). We have reported that RBM15, a primarily nuclear protein, also binds to the general mRNA export factor NXF1 (20), suggesting that RBM15 can tether the RTE-containing RNA to the NXF1 export pathway. In contrast to RTE, the constitutive transport element (CTE)-containing Mason-Pfizer monkey virus/simian retrovirus viral

* This work was supported, in whole or in part, by the National Institutes of Health Intramural Research Program.

Author's Choice—Final version full access.

§ The on-line version of this article (available at <http://www.jbc.org>) contains supplemental Fig. S1.

¹ Present address: Genentech, Inc., South San Francisco, CA 94080.

² Present address: Institute of Molecular and Cell Biology, Singapore 138673.

³ To whom correspondence should be addressed: P.O. Box B, Bldg. 535, Rm. 209, Frederick, MD 21702-1201. Tel.: 301-846-5159; Fax: 301-846-7146; E-mail: felberb@mail.nih.gov.

⁴ The abbreviations used are: RRM, RNA recognition motif; SPOC, Spen paralogue and orthologue C-terminal; SFC, splicing factor compartment; HE, heterozygous; HO, homozygous; NE, nuclear envelope; CTE, constitutive transport element; aa, amino acids; HIV-1, human immunodeficiency virus, type 1; CAT, chloramphenicol acetyltransferase; HA, hemagglutinin; GFP, green fluorescent protein; GST, glutathione S-transferase; En, embryonic day *n*; N-tagged, N-peptide-tagged.

RNAs are exported via direct binding of the CTE to the NXF1 nuclear export receptor (25). Thus, although both RTE and CTE promote export of viral RNAs using cellular factors, the detailed mechanism of function is thought to be distinct: CTE binds NXF1 directly, whereas RTE has the ability to interact with NXF1 via RBM15.

In this work, we examined the function of the human SPEN proteins OTT3, RBM15, and SHARP. We found that OTT3, like RBM15 but unlike SHARP, acts at the post-transcriptional level to activate reporter gene expression.

EXPERIMENTAL PROCEDURES

Recombinant DNA—The *gag* reporter plasmids pNLgag (22) and pNLgag-RTE (23) were described. pNLgag consists of the HIV-1 5' long terminal repeat and the 5'-untranslated region containing the major splice donor of HIV-1 followed by the *gag* gene (nucleotides 1–2621 of NL4-3 starting with the first nucleotide of U3 as +1) and the HIV-1 sequence from nucleotide 8886 (XhoI) to end of the 3' long terminal repeat (nucleotide 9709) including a cryptic splice acceptor. This plasmid produces an unspliced *gag*-encoding and spliced noncoding mRNA (22). The CAT reporter pDM128/B, the expression plasmids for NXF1, p15/NXT1, HA-tagged NXF1, FLAG-tagged RBM15, N-peptide-tagged RBM15, and GFP expression plasmid pF25 were described previously (20, 24–27). The OTT3-encoding plasmid pSG-OTT3 was obtained from E. Manet. For expression in *Escherichia coli*, OTT3 was inserted into pGEX-6P-3 (Amersham Biosciences). N-peptide-tagged OTT3 and its deletion mutants were generated by replacing NXF1 in pN-TAP plasmid (26). FLAG-tagged OTT3 was constructed by insertion of OTT3 in p3XFLAG-CMV-14 (Sigma). HA-tagged SHARP was obtained from R. A. Evans.

Cell Culture, Transfection, and Immunofluorescence—The HeLa-derived cell line HLtat produces the HIV-1 Tat protein necessary for the activation of the long terminal repeat promoter of the *gag* reporter plasmid; human 293 and 293T cells were transiently transfected using Superfect (Qiagen) or calcium coprecipitation (20). Gag (HIV p24gag antigen capture assay; Zeptomatrix), CAT activity, and GFP fluorescence were measured (20). For indirect immunofluorescence, the cells were fixed with 3.7% paraformaldehyde or cold methanol followed by permeabilization in 0.5% Triton X-100 (28). RBM15 polyclonal antibody (10587-1-AP; Proteintech), SC-35 mAb (SC-35; Sigma), HA epitope mAb (HA.11; Covance), and FLAG epitope mAb (M2; Sigma) were used as primary antibodies, followed by detection with Alexa-conjugated secondary antibodies (Molecular Probes, Eugene OR). In some experiments, the HA epitope was detected directly using fluorescein-conjugated HA antibodies (Roche Applied Science). The wide field epifluorescence images were acquired and processed as described (28). Image acquisition with ApoTome module was performed using Axio Observer microscope and AxioVision software (Carl Zeiss Microimaging).

Immunoprecipitation and In Vitro Binding Assays—For coimmunoprecipitation assays, 293 cells were transfected with 1–5 μ g of expression constructs and harvested at day 2 post-transfection. The cells were extracted in 150 mM NaCl in the presence of 0.2% Triton X-100 in a buffer containing also 15 mM

HEPES (pH 7.9), 0.1 mM EDTA, and 10% glycerol, treated with RNase A prior to immunoprecipitation with anti-FLAG-agarose (Sigma), and the complexes were eluted with 3 \times FLAG peptide (Sigma) or by boiling in SDS-PAGE loading buffer. For high stringency conditions, immunoprecipitations and subsequent washes were performed in the presence of 400 mM NaCl and 50 mM KCl, and the wash buffer was additionally supplemented with 2 M urea. *In vitro* protein binding assays were performed (28) using *E. coli*-expressed purified GST-tagged RBM15 and OTT3 and reticulocyte-produced NXF1 proteins.

Mice with *Ott1*^{XK135} Allele—The mouse ES cell line XK135 (obtained from BayGenomics; funded by the NHLBI, National Institutes of Health), harbors a LacZ-neo fusion cassette inserted into the first coding exon of *RBM15*, 20 nucleotides upstream the initiator codon, generating a hypomorphic *RBM15*^{XK135} allele. After injection into C57BL/6 blastocysts, the chimeric mice were bred for germline transmission. Genomic DNA from tail snips or yolk sacs was used for PCR genotyping. *RBM15* alleles were detected by PCR using primers that span the cassette insertion site.

mRNA Microarrays—Total RNA from the genotyped mouse embryos was analyzed on GE Healthcare CodeLinkTM mouse whole genome bioarrays. Expression data and detailed protocols have been deposited in the NCBI Gene Expression Omnibus (29) and are accessible through GEO accession number GSE11785. Because the existing normalization approaches were not applicable for data sets reflecting biologically relevant intensity-dependent differences (30), the expression data were not subject to intensity normalization. The biologically relevant groups of transcripts in expression data sets were evaluated using PANTHER tools.

Statistical Analyses—The expression data were evaluated using the Mann-Whitney two-sample rank sum test, with $\alpha = 0.05$. The embryonic genotype distributions were compared with the Mendelian distribution by using the χ^2 test. Data pruning was performed by averaging every 20 rows to produce one output row, using the GraphPad Prism software.

Bioinformatics—The amino acid sequences of SPEN superfamily proteins were compiled using Batch Entrez and BLAST utilities at NCBI. Multiple amino acid sequence alignments were performed using MAFFT software (31) and refined manually. Phylograms were drawn using BLOSUM62 distances and the unweighted pair group method using arithmetic averages and refined manually in Jalview alignment editor (32).

RESULTS

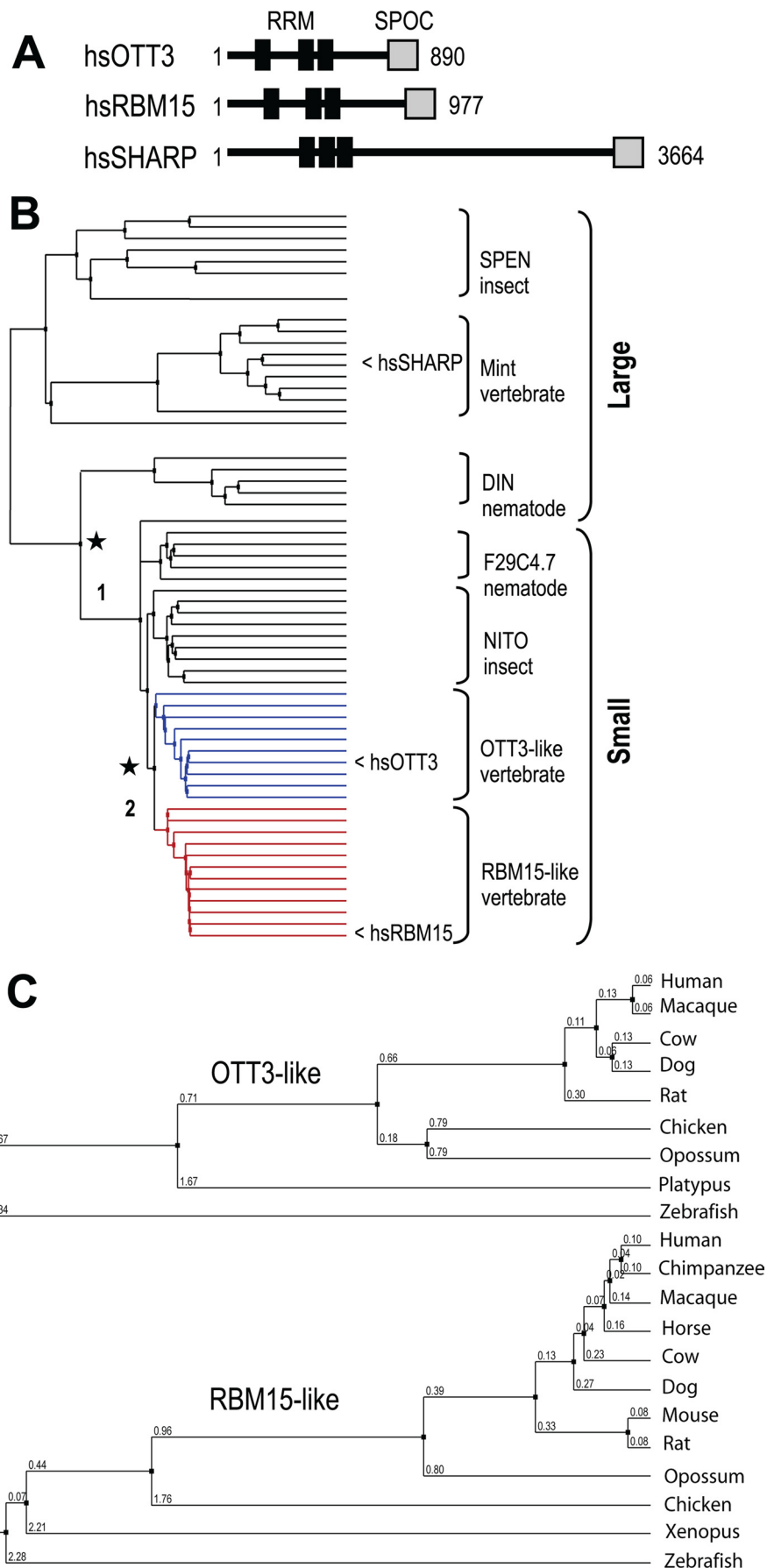
Molecular Phylogeny Suggests Distinct Roles of RBM15 and OTT3—The SPEN family proteins SHARP, RBM15, and OTT3 share the domain architecture comprising of three N-terminal RRM and a SPOC domain (1–3) (Fig. 1A). We used amino acid sequence alignments and molecular phylogeny to compare the SPEN proteins within and across species. This analysis suggested that the large and small proteins are separate classes that split before the existence of a common ancestor of nematodes and humans (Fig. 1B, node 1). Notably, the small SPEN proteins of vertebrates formed two distinct clusters across taxa that we termed RBM15-like and OTT3-like (Fig. 1B, node 2), whereas the small proteins of insects (NITO) and nematodes (F29C4.7)

OTT3 and RBM15 Function

were confined to taxa-specific clusters. In the RBM15-like and OTT3-like clusters, the branches were congruent with taxonomy (Fig. 1C), strongly supporting orthology within these groups. Thus, these data suggested a biologically relevant difference between OTT3 and RBM15 that is conserved in vertebrates.

OTT3 Promotes Export of the CAT Reporter mRNA via Its C-terminal Domain—We previously found that RBM15 acts at the post-transcriptional level and promotes export and expression of reporter transcripts (20). In this report, we tested OTT3 for such function using the DM128/B *cat* mRNA tethering assay (26) (Fig. 2). In this system, the reporter transcript contains the *cat* gene and the high affinity binding sites (Fig. 2A, box B) for the RNA-binding N-terminal domain of lambdaoid phage P22 antiterminator protein N (Fig. 2A, *N-peptide*). This reporter RNA is designed to be retained in the nucleus and hence expresses only background levels of CAT protein. Fusion of the N-peptide to a protein with mRNA export activity leads to its tethering to the DM128/B transcript, resulting in stimulation of CAT expression. Because the major expression defect of DM128/B transcript is due to inefficient nuclear export, CAT expression activation provides a read-out of mRNA export activity of the tethered protein. Cotransfection of the *cat* reporter with the untagged proteins, which cannot interact with the box B-containing *cat* transcript, serves as specificity control.

N-peptide fusions with OTT3 and deletions thereof were generated (Fig. 2B), and their expression was verified using indirect immunofluorescence of HA-tagged proteins (data not shown). Coexpression of the N-tagged full-length OTT3 with DM128/B revealed its RNA export activity (Fig. 2C). In parallel transfections, we found that N-tagged RBM15 as well as the N-tagged NXF1 activated CAT expression as expected (20, 26). No activation was observed upon coexpression of



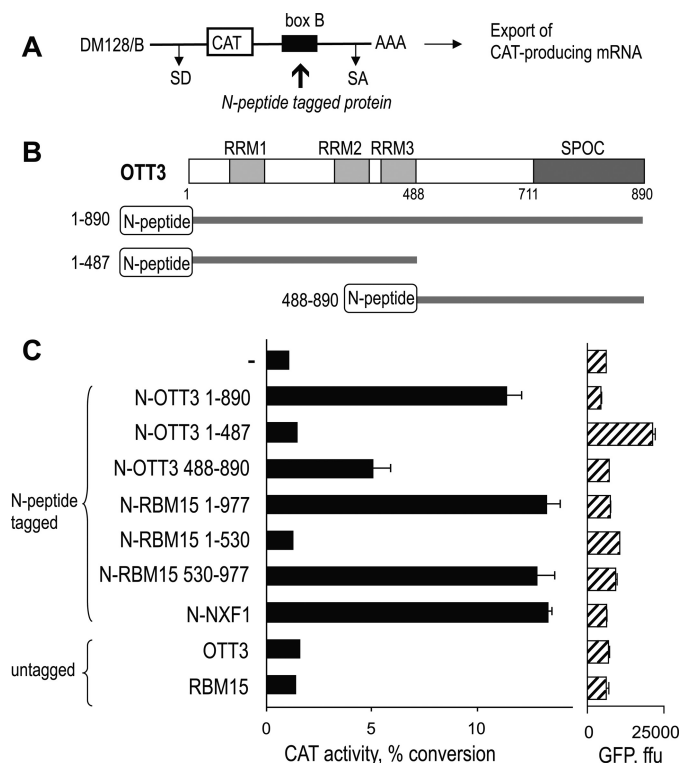


FIGURE 2. OTT3 stimulates *cat* mRNA expression when tethered to the transcript. *A*, tethering assay to detect nuclear export activity. CAT protein is only produced from DM128/B transcripts that are exported from the nucleus before splicing. Export can be activated when a N-tagged export factor is tethered to DM128/B via binding of the N-peptide moiety and its high affinity RNA ligand (box B) present within the intron of DM128/B. Stimulation of CAT production in the presence of a N-tagged protein provides a measure of its nuclear export activity. *B*, schematic of N-tagged OTT3 (aa 1–890) and of its mutants. N-OTT3 1–487 contains the RRM motifs and N-OTT3 488–890 includes the SPOC domain. To facilitate detection, these proteins also included HA epitope tags at the C terminus, and their expression was verified by Western blots using HA antibody. *C*, human 293 cells were transfected in duplicate with 0.02 μ g of pDM128B reporter plasmid alone (–) or together with 0.3 μ g of the indicated N-tagged OTT3 and RBM15 and, as positive control, the N-tagged NXF1 expression plasmids. As negative control, plasmids expressing untagged OTT3 and RBM15 were used. As internal control for transfection efficiency, all transfections included 0.5 μ g of GFP expression plasmid pFRED25. Two days post-transfection, CAT activity and GFP fluorescence were measured and are plotted on the x axis (CAT, % conversion; GFP, firefly units (ffu)). The mean values and standard errors of two independently transfected plates of a representative experiment are shown. The lack of error bars in some of the columns is due to very small differences that cannot be visualized in this scale.

OTT3 or RBM15 lacking the N-peptide, demonstrating that tethering to the transcript is essential for function and also shows that these proteins do not have transcriptional function. This assay further allows the dissection of the protein domains and allows a qualitative assessment of their activity. Fig. 2C shows that the C-terminal region spanning aa 488–890 of OTT3 is active, in contrast to the N-terminal region spanning aa 1–487, and this finding is in overall agreement with the reported properties of the domains of the related RBM15 (Fig. 2C) (20).

These data support the conclusion that OTT3 promotes the nuclear export of *cat* transcript, acting via its C-terminal region. Thus, OTT3 has mRNA export activity like previously reported

RBM15, NXF1, and HIV-1 Rev (20, 26). However, OTT3 does not shuttle between the nucleus and cytoplasm, pointing to its function as export cofactor rather than export receptor, similar to the reported role of RBM15 (20).

OTT3 Promotes Expression of the RTE-containing Reporter Transcript—We previously found that RBM15 recognizes the RNA export element RTE and activates RTE-mediated reporter gene expression (20), and here we tested OTT3 for similar function. The reporter NLgag mRNA encodes the HIV p55gag protein and produces only low levels of Gag protein, whereas the insertion of RNA export elements (*i.e.* CTE, RTE, and RRE) 3' to the *gag* gene promotes the export and expression of the unspliced *gag* reporter RNA (20, 22, 33–35). We expressed the empty NLgag and the RTE-containing NLgag-RTE (Fig. 3A) in human HeLa-derived HLtat cells, in the absence or presence of coexpressed SPEN proteins. We found that none of the SPEN proteins had an effect on empty NLgag, confirming the absence of nonspecific effects. These data further support the notion that the export factors need to interact specifically with the target transcript (see also Fig. 2). As expected, the presence of RTE in the gag-RTE transcript resulted in induction of Gag expression (20, 23). Interestingly, coexpression of OTT3 led to a further strong activation of expression of NLgag-RTE (Fig. 3A). Similarly, RBM15 promoted Gag expression from NLgag-RTE (20), whereas SHARP had no effect (Fig. 3A). These data demonstrated that, in contrast to SHARP, both OTT3 and RBM15 act as post-transcriptional activators (Figs. 2 and 3) and specifically activate the RTE-containing reporter RNA (Fig. 3). Together, OTT3 acts at post-transcriptional steps by (i) promoting expression of the RTE-containing reporter transcripts (Fig. 3), (ii) tethering the *cat* reporter to the export machinery (Fig. 2 and see below), and (iii) acting as splicing suppressor of a β -thalassemia transcript (19). Because SHARP is a transcription factor with no reported role in post-transcriptional regulation, we speculate that the precursors of SPEN proteins split into the large and small structural classes (Fig. 1B, node 1) because of functional specialization. It is plausible that the large proteins retained their original role in transcription, whereas the small proteins, like OTT3 and RBM15, evolved as post-transcriptional regulators. In support of these findings, the SPOC domain of SHARP was reported to have a much stronger transcriptional repression activity than those of RBM15 and OTT3 (19), which is consistent with the loss of transcription coregulator activity concomitant with the acquisition of post-transcriptional function.

OTT3 Acts as NXF1 Cofactor to Activate mRNA Expression—Because OTT3 is primarily a nuclear protein (19) (see Figs. 6 and 7), we next tested the possible cooperation between OTT3 with the nuclear export receptor NXF1. OTT3 and NXF1 were coexpressed with the *gag* reporter transcripts in the human 293T cell line that best allows study of the effects of NXF1 and its cofactor p15 (36, 37). Fig. 3B shows that coexpression of NXF1/p15 with OTT3 or RBM15 had no effect on the empty *gag* reporter. In contrast, NXF1/p15 further augmented the

FIGURE 1. Phylogenetic analysis of the SPEN protein family. *A*, schematic depicting the human SPEN family proteins OTT3, RBM15, and SHARP. RRM motifs (black) and SPOC domains (gray) are shown. *B*, phylogram showing the split between the small and large (node 1) and OTT3 (blue) and RBM15 (red) (node 2) SPEN proteins. *C*, enlarged branches from *B*. Node 2 shows taxonomy-congruent structures of the OTT3 and RBM15 clusters in vertebrates.

OTT3 and RBM15 Function

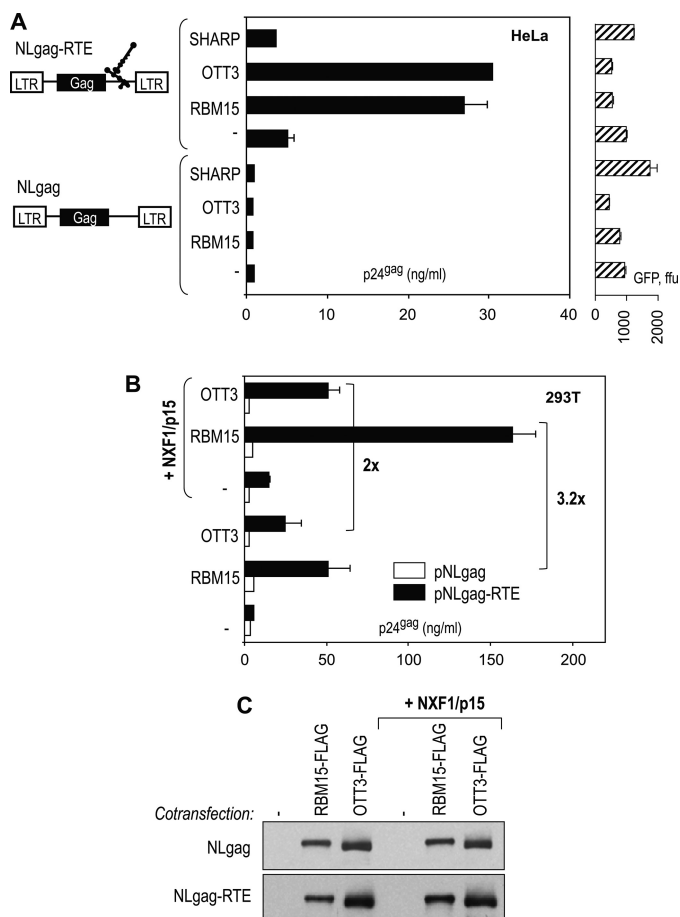


FIGURE 3. OTT3 activity is enhanced by the mRNA receptor NXF1. *A*, HeLa cells were transfected in triplicate with 1 μ g of reporter NLgag or NLgag-RTE plasmids alone (–) or together with 0.5 μ g of OTT3, RBM15, or SHARP expressing plasmids, as shown to the left of the panel. All transfections included 0.5 μ g of GFP expression plasmid pFRED25 that served as internal control of transfection efficiency. p24^{gag} antigen and GFP fluorescence were measured at day 2 post-transfection, and raw expression values (p24^{gag}, ng/ml; GFP, firefly units (ffu)) are plotted on the x axis. The mean values and standard deviation of three independently transfected plates of a typical experiment are shown. The lack of error bars in some of the columns is due to very small differences that cannot be visualized in this scale. *B*, human 293T cells were transfected in triplicate with 0.5 μ g of reporter NLgag or NLgag-RTE plasmids in the presence or absence of NXF1 (0.5 μ g) and p15/NXF1 (0.1 μ g) expression plasmids. All of the transfections included 0.1 μ g of HIV-1 Tat-expressing plasmid pBstat, necessary to activate expression from long terminal repeat (LTR) promoter. p24^{gag} antigen was measured at day 2 post-transfection, and raw expression values (p24^{gag}, ng/ml) are plotted on the x axis. The means and standard deviation of three independently transfected plates of a representative experiment are shown. *C*, Western blot analysis of OTT3-FLAG and RBM15-FLAG proteins from cells transfected as described for *A*.

OTT3-mediated expression from NLgag-RTE, suggesting cooperativity between OTT3 and NXF1. Similarly, NXF1/p15 activated the function of RBM15 (Fig. 3*B*), as reported previously (20). Notably, in 293T cells, there was a pronounced difference in the extent of gag reporter gene activation comparing OTT3 (5-fold) and RBM15 (10-fold), and dose dependence studies confirmed that it was due to the intrinsic properties of RBM15 and OTT3 rather than their expression levels (data not shown). In addition, coactivation of OTT3 by NXF1/p15 (2-fold) was reproducibly slightly weaker than that of RBM15 (~3-fold). To exclude the possibility that the difference was due to lower OTT3 expression, we performed Western blot analysis using the extracts from the experiments shown in Fig. 3*B*,

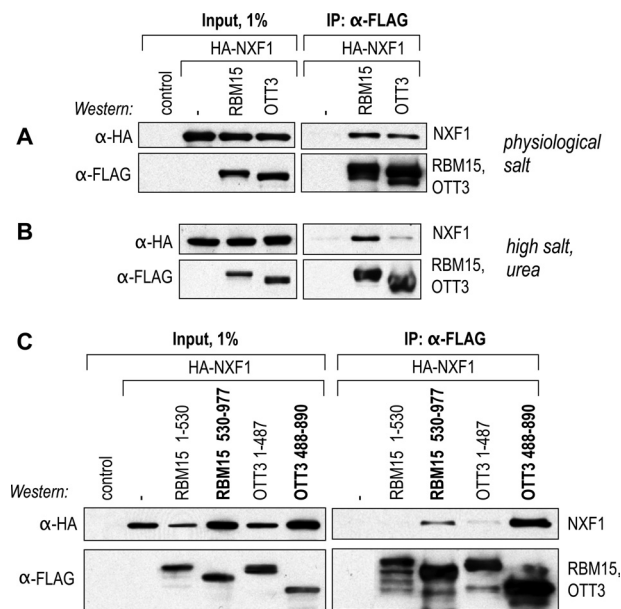


FIGURE 4. OTT3 associates with NXF1 in vivo. Human 293 cells were transfected with HA-tagged NXF1 in the absence or presence of plasmids expressing FLAG-tagged intact OTT3 or RBM15 (*A* and *B*) or N- and C-terminal mutants of RBM15 and OTT3 (*C*). Coimmunoprecipitations were performed using anti-FLAG agarose in the presence of physiological conditions using 150 mM NaCl (*A* and *C*) or high salt using 400 mM NaCl, 50 mM KCl, and 2 M urea (*B*). The epitope-tagged proteins were analyzed in 1% aliquots of raw extracts (*Input*). The FLAG-immunoprecipitated (*IP*) complexes were visualized using Western immunoblot analysis. OTT3 and RBM15 proteins were detected with α -FLAG antibody, and the pulled down NXF1 was detected with α -HA antibodies. *control*, untransfected cells. The lower band of OTT3, pulled down on the FLAG-beads under physiological conditions (*A*, right panel), likely represents a degradation product.

which revealed that OTT3 was expressed to even higher levels than RBM15 (Fig. 3*C*). Taken together, these results demonstrate the ability of OTT3 to cooperate with NXF1 in the activation of the RTE-mediated reporter gene expression and further indicate that in some cell types OTT3 function is intrinsically weaker than that of RBM15.

OTT3 Interacts with NXF1 in Vivo—The activation of OTT3 by NXF1 suggests interaction of the factors, and thus, we tested OTT3 for its ability to bind to NXF1. We performed coimmunoprecipitations (Fig. 4) from extracts of human 293 cells that expressed FLAG-tagged OTT3 together with HA-tagged NXF1. As control, we also transfected FLAG-tagged RBM15, which we previously reported to interact with NXF1 (20). To ensure that only RNA-independent interactions were analyzed, the extracts were pretreated with RNase A. Western blots verified the expression of HA-NXF1 as well as of OTT3 and RBM15 (Fig. 4, *A* and *B*, *Input*). Immunoprecipitations (Fig. 4*A*) using anti-FLAG antibody revealed that NXF1 coprecipitated efficiently and specifically with FLAG-OTT3 at physiological ionic strength (150 mM NaCl). Interestingly, under high stringency conditions (400 mM NaCl, 50 mM KCl, 2 M urea), coimmunoprecipitation of OTT3 with NXF1 was less efficient, whereas the RBM15-NXF1 association was not changed significantly (Fig. 4*B*). These data provided evidence of a differential interaction of NXF1 with OTT3 and RBM15, respectively, which likely reflects the intrinsic molecular properties of proteins rather than their availability to interact (*e.g.* overall expression levels). These data suggested that the reduced activ-

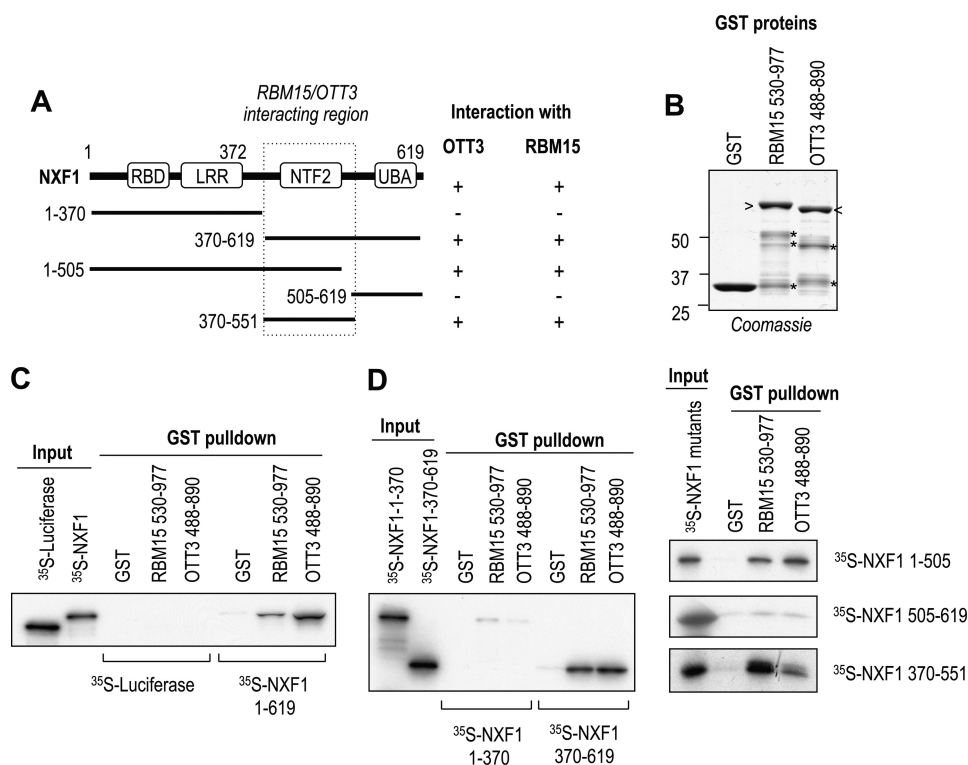


FIGURE 5. In vitro binding of NXF1 to OTT3 and RBM15. A, schematic of the NXF1 deletion mutants and summary of the *in vitro* binding data. Proteins representing functional domains of NXF1 were expressed and metabolically labeled in reticulocyte extracts and tested for binding to *E. coli*-produced purified GST-OTT3 and GST-RBM15 proteins representing their C-terminal regions. B, expression of the recombinant proteins GST-OTT3 (488–890) and GST-RBM15 (530–977). Arrowheads, full-length; asterisks, truncated forms. C and D, GST pull-downs of ³⁵S-radiolabeled reticulocyte-produced NXF1 and its mutants. In C, firefly luciferase protein (³⁵S-Luciferase) is also included, as binding specificity control. The ³⁵S-radiolabeled proteins (10% aliquots of input fractions) and the GST pull-downs were analyzed by SDS-PAGE and visualized by radiofluorography.

ity of OTT3 could be due in part to its weaker interactions with NXF1 (Fig. 3).

Our previous work showed that the C-terminal region of RBM15 binds to NXF1 and suggested that this interaction is key to RBM15 activity (20). We therefore tested FLAG-tagged OTT3 deletion mutants for their association with HA-tagged NXF1 (Fig. 4C, mutants containing the C-terminal regions are indicated in *bold type*). These experiments revealed that OTT3 interacted with NXF1 via its C-terminal region (aa 488–890), similarly to RBM15. We noted that, in contrast to the full-length protein, the isolated C-terminal region of OTT3 was able to pull-down NXF1 more efficiently than that of RBM15 (Fig. 4C). Collectively, these data demonstrated that NXF1 binds both OTT3 and RBM15 via their C-terminal regions and that NXF1 is able to discriminate between these two proteins.

OTT3 Interacts with NXF1 in Vitro—To further address the specificity of the interactions of OTT3 and RBM15 with NXF1, we performed *in vitro* binding studies to map their interacting regions within NXF1. The full-length NXF1 and its deletion mutants were produced as outlined in Fig. 5A and metabolically labeled using reticulocyte extracts. These proteins were used in GST pull-down assays together with recombinant OTT3 and RBM15 proteins spanning the C-terminal regions (Fig. 5B). To exclude the RNA-mediated interactions, binding reactions were performed in the presence of RNase A. We found that OTT3 interacted specifically with the full-length NXF1, as

reported for RBM15 (20), but not luciferase, which served as a negative control, and OTT3 bound more efficiently than RBM15 (Fig. 5C), consistent with the *in vivo* data (Fig. 4C). Fig. 5D shows the mapping of the binding domain within NXF1 by testing regions spanning aa 1–370 and 370–619 (*left panel*) and aa 1–505, 505–619, and 330–551 (*right panel*), and the data are summarized in Fig. 5A. No interaction was found with NXF1 aa 1–370, whereas aa 370–619 interacted efficiently (*left panel*). Analysis of additional NXF1 deletion mutants showed that the C-terminal aa 505–619 (*right panel*) did not interact, whereas the N-terminal region of NXF1, aa 1–505, interacted with OTT3 and RBM15, indicating that the region spanning aa 370–551, which contains the NXF1 NTF2-like domain (Fig. 5A), harbors the domain necessary for binding. Indeed, testing of the NXF1 region (aa 370–551) confirmed interaction with both OTT3 and RBM15 (Fig. 5D, *right panel*).

Taken together, these results established that NXF1 bound *in vitro* to the C-terminal regions of

RBM15 and OTT3 via its NTF2-like domain (aa 370–551), whereas our *in vivo* studies suggest that the C-terminal region of OTT3 has an intrinsically reduced interaction with NXF1 compared with RBM15, which may explain its lower functional activity observed in transfected human 293T cells (Fig. 3B).

RBM15 and OTT3 Associate with NXF1 Cofactor Aly/REF in Vivo—By screening known NXF1 cofactors using coimmunoprecipitation assays, we found that OTT3 and RBM15 also associated with Aly/REF, a RNA-binding factor that was implicated in the assembly of NXF1 with export-ready mRNP complexes, serving as a link between pre-mRNA splicing and mRNA export (38–42). We tested the interaction of OTT3 and RBM15 with the REF variants REF1-II and REF2-II, which differ by the presence of an N-terminal variable region (Fig. 6A). Coprecipitation of HA-tagged REF2-II (Fig. 6B) with FLAG-tagged OTT3 and RBM15 revealed an interaction of REF2-II with both RBM15 and OTT3. Pull-down experiments using recombinant proteins further revealed that REF2-II interacts with the C-terminal portions of OTT3 and RBM15 (data not shown), which also contain the interaction sites with NXF1 (Fig. 5). In contrast, REF1-II did not coprecipitate efficiently with RBM15 or OTT3 (data not shown).

We next compared the subcellular localization of GFP-tagged REF2-II in the absence or presence of cotransfected HA-tagged OTT3 and RBM15 in HeLa cells (Fig. 6C). REF2-II was found in the nucleoplasm and was enriched in nuclear speckles

OTT3 and RBM15 Function

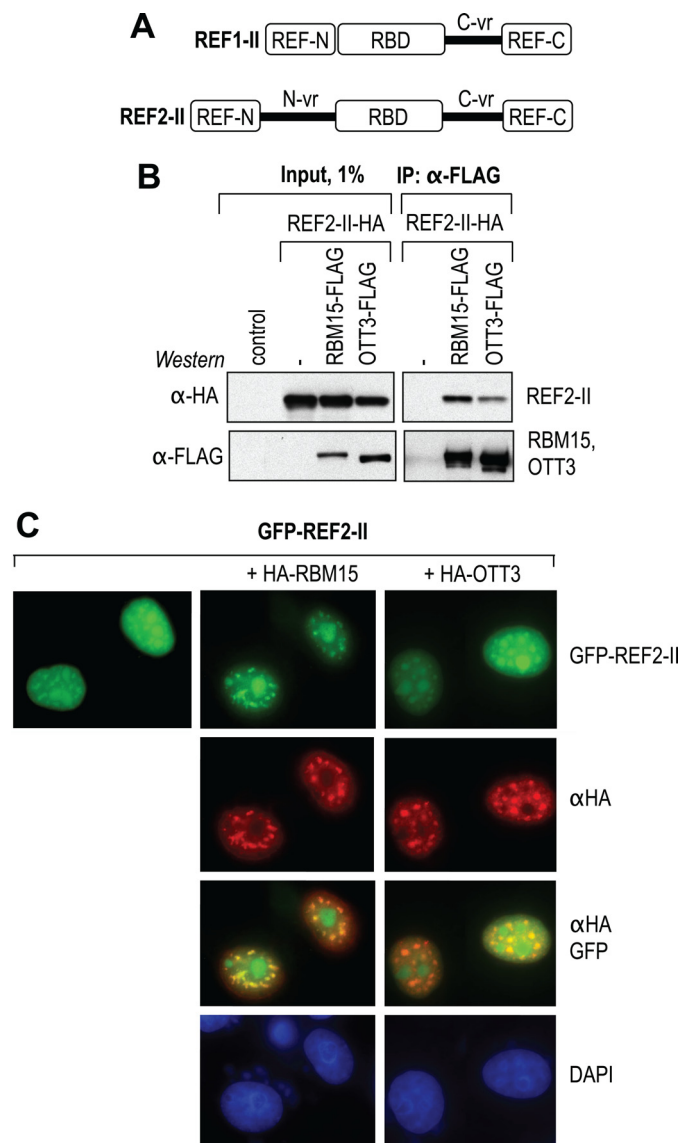


FIGURE 6. OTT3 and RBM15 interact with Aly/REF. *A*, schematic depicts the domain structure of REF1-II and REF2-II proteins. *B*, association of OTT3 and RBM15 with REF2-II *in vivo*. Coimmunoprecipitation assays were performed in RNase A-treated extracts under using 150 mM NaCl as described for Fig. 4. *C*, the GFP-REF2-II was expressed in HeLa cells alone or in the presence of HA-tagged RBM15 or OTT3. After paraformaldehyde fixation and Triton X-100 permeabilization, the SPEN proteins were visualized by indirect immunofluorescence with HA antibodies, and REF2-II was detected by GFP fluorescence.

reported to represent SFC as expected (38, 43). REF2-II also accumulated in the nucleoli, which could be attributed to its nonspecific association with RNA in this compartment, and these effects were not further addressed. Coexpression of REF2-II with OTT3 and RBM15, respectively, showed extensive colocalization (Fig. 6C). REF2-II, OTT3, and RBM15 proteins were enriched in SFC, in agreement with our data in Fig. 7A (staining with anti-SC35 antibody). In contrast, REF1-II did not colocalize with OTT3 and RBM15 (data not shown), supporting our biochemical data that showed the selective binding of OTT3 and RBM15 to REF2-II but not to REF1-II. Because REF2-II mostly differs from REF1-II by the presence of a N-terminal variable region (Fig. 6A), it is plausible that this region

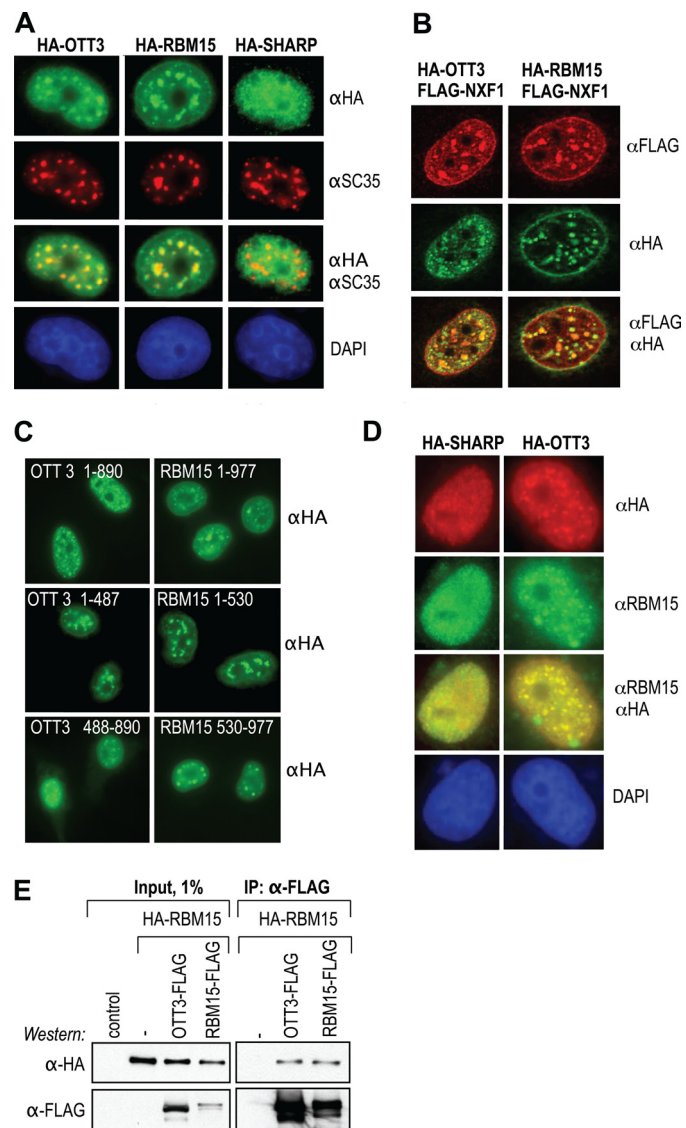


FIGURE 7. OTT3 and RBM15 associate with the nuclear envelope and SFC and form complexes *in vivo*. HeLa cells expressing the indicated epitope-tagged proteins were subject to indirect immunofluorescence. *A*, dual-color detection of the exogenously expressed HA-tagged SPEN proteins and endogenous SC35 antigen. The cells were counterstained with nuclear dye 4',6-diamidino-2-phenylindole (DAPI). *B*, dual-color detection of the exogenously expressed HA-tagged OTT3 and RBM15 proteins and FLAG-tagged NXF1. The images were acquired using ApoTome module (Carl Zeiss Microimaging). *C*, single-color detection of FLAG-tagged OTT3 and RBM15 proteins and their deletion mutants. *D*, dual-color detection of the exogenously expressed HA-tagged SPEN proteins OTT3 and SHARP and the endogenous RBM15. Raw, unfiltered images of representative fields are shown, depicting equatorial sections of the nuclei. The cells were counterstained with nuclear dye 4',6-diamidino-2-phenylindole. *E*, coimmunoprecipitation of OTT3 with RBM15. Human 293 cells were transfected as indicated, and proteins were detected on Western blots in 1% aliquots of raw extracts (*Input*) and in OTT3-FLAG and RBM15-FLAG complexes that were immunoprecipitated with FLAG antibodies (*IP: α-FLAG*). *Control*, untransfected cells. Representative experiments are shown, and similar data were obtained in three independent experiments.

contributed to both the localization of REF2-II with SFC and its affinity to OTT3 and RBM15. Together, these data revealed highly selective interactions of both small SPEN proteins with the mRNA export factor REF2-II that acts upstream of NXF1, further supporting our model that OTT3, like RBM15, is an integral part of the NXF1 pathway.

Distinct Subcellular Localization of OTT3—To examine possible differences between the human SPEN proteins, we first compared their subcellular localization upon transfection of HA-tagged proteins into HeLa cells. We found that HA-OTT3 and HA-RBM15 accumulated strongly in nuclear speckles (Fig. 7A). Staining with anti-SC35 antibody showed that these speckles were positive for SC35 antigen and hence represented the SFC (Fig. 7A). For RBM15, this location is expected based on the previous characterization of RBM15 as a spliceosome-associated protein (44). In contrast, HA-SHARP formed a finely punctate pattern in the nucleoplasm as previously published (10) and was not enriched in the SFC or at the nuclear envelope (NE) (Fig. 7A), further supporting a distinct biological function of the large member of the SPEN family.

For a more detailed analysis, we compared the localization of HA-OTT3 and HA-RBM15 with that of NXF1, a known NE-associated protein (24, 45, 46). To facilitate detection, NXF1 was tagged with the FLAG epitope. We found that FLAG-NXF1 was present at the NE as expected (24, 45) (Fig. 7B) and that it was also found in nuclear speckles that represent the SFC (data not shown). Both HA-RBM15 and HA-OTT3 were also prominently enriched in SFC in agreement with the data shown in Fig. 7A. In addition, HA-RBM15 accumulated at the NE, like FLAG-NXF1, whereas HA-OTT3 was mostly present in the nucleoplasm and was barely detectable at the NE (Fig. 7B).

To understand whether these differences were due to intrinsic properties of the OTT3 NE localization signal, we tested the FLAG-tagged deletion mutants of OTT3 and RBM15 for NE association (Fig. 7C). We found that the isolated N-terminal portions of RBM15 (aa 1–530) and OTT3 (aa 1–487) contain NE localization signals, whereas their C-terminal portions (RBM15, aa 530–977; OTT3, aa 488–890) localized to the nucleoplasm. Notably, in contrast to the full-length proteins (Fig. 7C, top row; see also Fig. 7, A and B), the isolated N-terminal portions of both OTT3 and RBM15 associated with the nuclear envelope with comparable efficiencies (Fig. 7C, middle row). These analyses revealed that the N-terminal regions of both proteins contain NE localization signals of similar strength but that this signal is less accessible within the full-length OTT3 protein. Collectively, these data led us to conclude that OTT3 and RBM15 localized similarly within the cell (nucleus; SFC association; NXF1 association) but that RBM15 accumulated more strongly at the nuclear envelope.

OTT3 and RBM15 Are Present in the Same Complexes in Vivo—Because OTT3 and RBM15 colocalize at the SFC (Fig. 7A), we asked whether they can interact with each other. We tested the colocalization of endogenous RBM15 and HA-tagged OTT3 and used as negative control HA-tagged SHARP. We found that the endogenous RBM15 efficiently colocalized with OTT3 (Fig. 7D) and was found enriched in the SFC compartment as identified in Fig. 7A. HA-tagged SHARP did not colocalize with the endogenous RBM15 (Fig. 8A). These data strongly suggest that RBM15 and OTT3 could be part of the same complexes in vivo. We tested this possibility by performing coimmunoprecipitation assays from extracts of cells that expressed HA-RBM15 alone or in combination with FLAG-

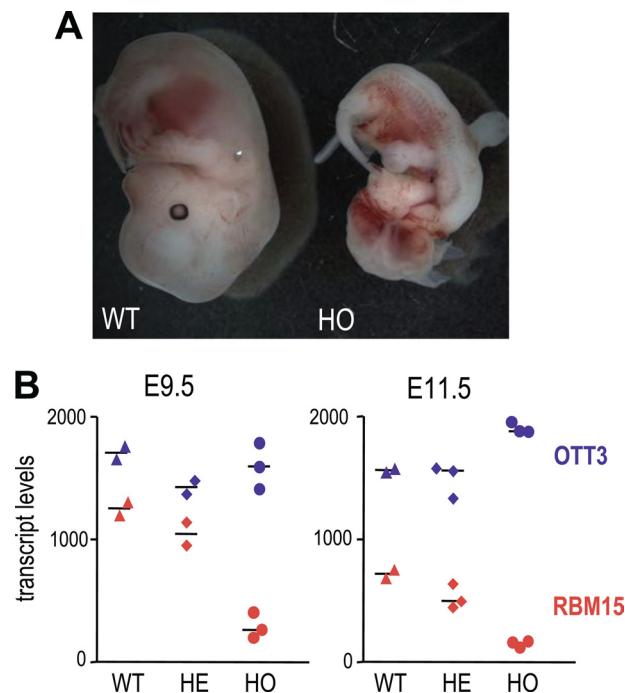


FIGURE 8. OTT3 cannot replace RBM15 function. *A*, mouse embryos at E11.5. *B*, levels of transcripts encoding RBM15 (red) and its homologue OTT3 (blue) were analyzed using mRNA microarrays (CodeLink, mouse whole genome bioarray, 36K), and the raw values for individual embryos (levels) are plotted on the y axis as intensity units. WT, wild type.

OTT3 or FLAG-RBM15 (Fig. 7E). To exclude the RNA-mediated interactions, extracts were pretreated with RNase A. Fig. 7E shows that precipitation with the anti-FLAG antibody revealed both the RBM15-RBM15 association as well as the RBM15-OTT3 association. These data support the existence of mixed complexes *in vivo*.

Essential Role of RBM15 in Mouse—We found that the small human SPEN proteins promote the nuclear export and expression of reporter *gag* and *cat* transcripts, suggesting that they could be involved in cellular mRNA metabolism. Because no lethal alleles or RNA interference were described for RBM15 or OTT3 orthologues *nito* (*D. melanogaster*) and F29C4.7 (*C. elegans*), we used mouse genetic knock-outs for studies on the organismal level. We focused on RBM15, because an ES cell line was available harboring a low expression allele (*RBM15*^{XK135}). We generated mice with the *RBM15*^{XK135} allele and found that heterozygous (HE) embryos and adults had no phenotype, whereas homozygous (HO) embryos died by embryonic day 12.5 (E12.5). We noted that using *RBM15*^{XK135} led to a slightly extended lifespan of the HO knockdown embryos, compared with mice homozygous for the previously described *RBM15* null allele (16) that had a lifespan of E9.5–10.5. At E11.5, the HO, but not HE embryos, showed reduction of body mass, abnormal organogenesis, and macroscopic superficial hemorrhages (Fig. 8A). We compared the levels of RBM15 and OTT3 RNA at E9.5 and 11.5 of two of three embryos with wild type, HE, and HO genotype (Fig. 8B). Quantification of the RBM15 transcript levels showed a ~5-fold reduction in the HO embryos compared with the wild type mice at both E9.5 and E11.5 (Fig. 8B, red symbols). We noted that homozygosity did not lead to a complete elimination of the *RBM15* transcripts,

OTT3 and RBM15 Function

verifying that *RBM15*^{XK135} was a low expression and not a null allele (Fig. 8B). In contrast, heterozygous mice (HE) showed only a 1.3-fold reduction (Fig. 8B) and displayed an absence of developmental, growth, or aging phenotypes. Importantly, the *OTT3* transcript levels were not affected significantly in the HO or HE animals (Fig. 8B, blue symbols), confirming that the *RBM15* knockdown phenotype developed on the wild type *OTT3* background. Because in our cell culture assays both the human *OTT3* and *RBM15* exhibited similar activities, we cannot exclude the possibility that the mouse *OTT3* complemented to some extent the *RBM15* loss of function, consistent with the lack of early embryonic phenotypes. It is also possible that besides sharing this basic activity, the two factors are involved in the regulation of distinct subsets of transcripts, thus serving nonredundant roles on the organismal level.

To gain further insight into the effects of the *RBM15* knockdown on cellular transcripts, we performed genome-wide studies of mRNA expression in total embryos. The supplemental Fig. S1 presents the results of our mRNA microarray analyses comparing wild type ($n = 2$), HE ($n = 3$), and HO ($n = 3$) embryos at E11.5 and illustrates the response of mouse transcripts to *RBM15* depletion in HO embryos. Most notably, we observed a massive up-regulation of low abundance mRNAs (supplemental Fig. S1A) in HO but not HE animals. Using the Mann-Whitney test to evaluate the response values for low abundance mRNAs, we found that a great number of such transcripts ($n = 15184$) were significantly up-regulated in HO but not HE embryos ($p = 0.0001$, $\alpha = 0.05$) (supplemental Fig. S1B). The observed inverse proportionality of response to expression level (supplemental Fig. S1B) was previously noted for global RNA phenotypes, but the reason for this bias is not well understood (47). The major affected gene category was G protein-coupled receptors (up-regulation, $n = 589$, $p = 2.00E-12$) (supplemental Fig. S1C), probably reflecting the very low abundance of G protein-coupled receptor transcripts in most tissues (48). RNA phenotypes were undetectable at day E9.5, in agreement with the absence of macroscopic phenotype, and the expressivity of both the macroscopic and RNA phenotypes varied between individual embryos, which could be attributed to variations in times of conception, and similar results were obtained when studying the *RBM15*^{XK135} allele in mice with different genetic backgrounds (data not shown). Together, these data established that *RBM15* depletion had a strong, global effect on mRNA expression, suggesting an important role for *RBM15* in gene expression regulation. In agreement with these data, recent work by others (16, 18) showed that *RBM15* nullisomy led to dysregulation in hematopoietic developmental pathways and cardiac malformation. The following mechanisms are compatible with the RNA phenotypes observed in *RBM15*^{XK135} homozygotes: (i) 50% reduction of essential redundant activity shared by *RBM15* and *OTT3* proteins, because of the loss of *RBM15* expression; (ii) trans-dominant negative effects of *OTT3* upon loss of *RBM15* expression; and (iii) loss of essential nonredundant *RBM15* activity. We noted that our studies of the small human SPEN proteins lend support to the mechanisms such as shared post-transcriptional regulatory activity and *RBM15*-*OTT3* association and recruitment *in vivo*. Our phylogenetic data point to the mechanism of diversi-

fication indicative of functional specialization. In summary, we concluded that *RBM15* is essential for mouse embryonic development, and the wild type expression levels of *OTT3* cannot compensate for its loss.

DISCUSSION

The SPEN family had diversified in the course of evolution, giving rise to three clearly orthologous groups in vertebrates that are represented by SHARP, *RBM15*, and *OTT3* in humans, and recent work has linked the “small” *RBM15* and *OTT3* proteins to post-transcriptional gene control. Unbiased approaches such as yeast two-hybrid screens and RNA pull-downs from crude extracts led to the characterization of *OTT3* as a binding partner of Epstein-Barr virus mRNA export factor EB2 (19); and *RBM15*, as a factor mediating the activity of the essential retroviral RNA export element RTE (20, 21). We previously showed that *RBM15* physically interacts and functionally cooperates with the general mRNA export receptor NXF1, suggesting a mechanism in which *RBM15* acts to tether RTE-containing RNA to NXF1 for export (20). Here, we found that *OTT3* also acts as export cofactor for the NXF1 export machinery.

In this study, an extensive comparison between *OTT3* and *RBM15* revealed a high degree of similarity in all aspects including functional activity, biochemical interactions, and subcellular targeting of these proteins, consistent with their structural relatedness. However, our phylogenetic studies indicated that *OTT3* and *RBM15* belong to orthologous groups that had diversified before the existence of the common ancestor of vertebrates, strongly suggesting a conserved, biologically relevant difference in function. In this work, we found that, in most, if not all assays used, *OTT3* displayed properties that are best described as attenuated in comparison with those of *RBM15*. Notably, *OTT3* interacted with the mRNA export receptor NXF1 but to a lesser extent than *RBM15*. This distinct interaction may be key to the reduced function of *OTT3* in some cell types. In support of this, the genetic knockdown of *RBM15* showed an embryonal lethal phenotype, indicating the *OTT3* could not complement the defect. Given the systemic nature of these differences, they plausibly reflect the relevant function that distinguishes the two paralogues, suggesting that *OTT3* evolved as an attenuated or/and specialized counterpart of *RBM15*. A compelling analogy exists to the NXF family factors, which, in metazoan species, include one essential member, the NXF1 orthologue responsible for the basic mRNA export, as well as one or more auxiliary NXFs that had diversified to serve more specialized roles (28, 49–54). In particular, neuronal roles were proposed for the human NXF5 and its putative mouse counterpart mNXF7. Interestingly, mNXF7 retains a full complement of subcellular localization signals typical of NXF factors including the nuclear localization signal and nuclear pore complex targeting determinants (49), yet these signals are overridden by a stronger determinant that is unique for mNXF7 and targets the protein to cytoplasmic mRNA transport granules (28). Likewise, the cryptic appearance of nuclear pore complex-targeting signal in *OTT3* may reflect the prevalence of its *e.g.* SFC-targeting signal, resulting in its depletion from the nuclear pore complex at steady state.

Why have vertebrates evolved and maintained the “strong” and “weak” variants of the otherwise similar factors? Because RBM15 and OTT3 are factors of the NXF1 pathway that controls the export of general mRNA, we speculated that they may be part of a developmental or/and tissue-specific switch that controls mRNA export rates or/and specificity. Extending the analogy between the NXF and SPEN families, a tissue-specific switch function has been ascribed for human NXF2 (24, 49, 55), another auxiliary NXF factor that was implicated in cytoplasmic mRNA metabolism and may have neuronal and male germ line-specific roles (51, 56). NXF2 acts in cooperation with its binding partner, fragile X mental retardation protein (56) to reduce the levels of NXF1 via destabilizing NXF1 mRNA (50), and hence this switch operates by physical replacement of the ubiquitous NXF1 with its tissue-specific counterpart. Further studies are needed to address the existence of similar RBM15/OTT3-operated switches. In summary, our work demonstrated an overall functional similarity between the small SPEN proteins and revealed a conserved difference in function that likely explains their divergence.

Acknowledgments—We thank E. Manet, E. Izaurralde, B. R. Cullen, T. R. Reddy, M. L. Hammarshjöld, D. Rekosh, and R. A. Evans for materials; G. Pilkington for discussions; and T. Jones for editorial assistance.

REFERENCES

- Kuang, B., Wu, S. C., Shin, Y., Luo, L., and Kolodziej, P. (2000) *Development* **127**, 1517–1529
- Rebay, I., Chen, F., Hsiao, F., Kolodziej, P. A., Kuang, B. H., Laverty, T., Suh, C., Voas, M., Williams, A., and Rubin, G. M. (2000) *Genetics* **154**, 695–712
- Wiellette, E. L., Harding, K. W., Mace, K. A., Ronshaugen, M. R., Wang, F. Y., and McGinnis, W. (1999) *Development* **126**, 5373–5385
- Kuroda, K., Han, H., Tani, S., Tanigaki, K., Tun, T., Furukawa, T., Taniguchi, Y., Kurooka, H., Hamada, Y., Toyokuni, S., and Honjo, T. (2003) *Immunity* **18**, 301–312
- Oswald, F., Kostecka, U., Astrahantseff, K., Bourteele, S., Dillinger, K., Zechner, U., Ludwig, L., Wilda, M., Hameister, H., Knöchel, W., Liptay, S., and Schmid, R. M. (2002) *EMBO J.* **21**, 5417–5426
- Oswald, F., Winkler, M., Cao, Y., Astrahantseff, K., Bourteele, S., Knöchel, W., and Borggreffe, T. (2005) *Mol. Cell. Biol.* **25**, 10379–10390
- Schreiber, S. L., Preiss, A., Nagel, A. C., Wech, I., and Maier, D. (2002) *Genesis* **33**, 141–152
- Lin, H. V., Doroquez, D. B., Cho, S., Chen, F., Rebay, I., and Cadigan, K. M. (2003) *Development* **130**, 3125–3135
- Doroquez, D. B., Orr-Weaver, T. L., and Rebay, I. (2007) *Mech. Dev.* **124**, 792–806
- Shi, Y., Downes, M., Xie, W., Kao, H. Y., Ordentlich, P., Tsai, C. C., Hon, M., and Evans, R. M. (2001) *Genes Dev.* **15**, 1140–1151
- Mercher, T., Coniat, M. B., Monni, R., Mauchauffe, M., Nguyen Khac, F., Gressin, L., Mugneret, F., Leblanc, T., Dastugue, N., Berger, R., and Bernard, O. A. (2001) *Proc. Natl. Acad. Sci. U.S.A.* **98**, 5776–5779
- Ma, X., Renda, M. J., Wang, L., Cheng, E. C., Niu, C., Morris, S. W., Chi, A. S., and Krause, D. S. (2007) *Mol. Cell. Biol.* **27**, 3056–3064
- Cen, B., Selvaraj, A., Burgess, R. C., Hitzler, J. K., Ma, Z., Morris, S. W., and Prywes, R. (2003) *Mol. Cell. Biol.* **23**, 6597–6608
- Chang, J. L., Lin, H. V., Blauwkamp, T. A., and Cadigan, K. M. (2008) *Dev. Biol.* **314**, 100–111
- Jemc, J., and Rebay, I. (2006) *Genetics* **173**, 279–286
- Raffel, G. D., Mercher, T., Shigematsu, H., Williams, I. R., Cullen, D. E., Akashi, K., Bernard, O. A., and Gilliland, D. G. (2007) *Proc. Natl. Acad. Sci. U.S.A.* **104**, 6001–6006
- Yabe, D., Fukuda, H., Aoki, M., Yamada, S., Takebayashi, S., Shinkura, R., Yamamoto, N., and Honjo, T. (2007) *Genesis* **45**, 300–306
- Raffel, G. D., Chu, G. C., Jesneck, J. L., Cullen, D. E., Bronson, R. T., Bernard, O. A., and Gilliland, D. G. (2009) *Mol. Cell. Biol.* **29**, 333–341
- Hiriart, E., Gruffat, H., Buisson, M., Mikaelian, I., Keppler, S., Meresse, P., Mercher, T., Bernard, O. A., Sergeant, A., and Manet, E. (2005) *J. Biol. Chem.* **280**, 36935–36945
- Lindtner, S., Zolotukhin, A. S., Uranishi, H., Bear, J., Kulkarni, V., Smulevitch, S., Samiotaki, M., Panayotou, G., Felber, B. K., and Pavlakis, G. N. (2006) *J. Biol. Chem.* **281**, 36915–36928
- Zolotukhin, A. S., Schneider, R., Uranishi, H., Bear, J., Tretyakova, I., Michalowski, D., Smulevitch, S., O’Keefe, S., Pavlakis, G. N., and Felber, B. K. (2008) *Virology* **377**, 88–99
- Felber, B. K., Hadzopoulou-Cladaras, M., Cladaras, C., Copeland, T., and Pavlakis, G. N. (1989) *Proc. Natl. Acad. Sci. U.S.A.* **86**, 1495–1499
- Nappi, F., Schneider, R., Zolotukhin, A., Smulevitch, S., Michalowski, D., Bear, J., Felber, B. K., and Pavlakis, G. N. (2001) *J. Virol.* **75**, 4558–4569
- Bear, J., Tan, W., Zolotukhin, A. S., Taberner, C., Hudson, E. A., and Felber, B. K. (1999) *Mol. Cell. Biol.* **19**, 6306–6317
- Grüter, P., Taberner, C., von Kobbe, C., Schmitt, C., Saavedra, C., Bachi, A., Wilm, M., Felber, B. K., and Izaurralde, E. (1998) *Mol. Cell* **1**, 649–659
- Wiegand, H. L., Lu, S., and Cullen, B. R. (2003) *Proc. Natl. Acad. Sci. U.S.A.* **100**, 11327–11332
- Stauber, R. H., Horie, K., Carney, P., Hudson, E. A., Tarasova, N. I., Gaitanaris, G. A., and Pavlakis, G. N. (1998) *BioTechniques* **24**, 462–466, 468–471
- Tretyakova, I., Zolotukhin, A. S., Tan, W., Bear, J., Propst, F., Ruthel, G., and Felber, B. K. (2005) *J. Biol. Chem.* **280**, 31981–31990
- Edgar, R., Domrachev, M., and Lash, A. E. (2002) *Nucleic Acids Res.* **30**, 207–210
- Wu, W., Dave, N., Tseng, G. C., Richards, T., Xing, E. P., and Kaminski, N. (2005) *BMC Bioinformatics* **6**, 309
- Katoh, K., Kuma, K., Toh, H., and Miyata, T. (2005) *Nucleic Acids Res.* **33**, 511–518
- Clamp, M., Cuff, J., Searle, S. M., and Barton, G. J. (2004) *Bioinformatics* **20**, 426–427
- Smulevitch, S., Bear, J., Alicea, C., Rosati, M., Jalah, R., Zolotukhin, A. S., von Gegerfelt, A., Michalowski, D., Moroni, C., Pavlakis, G. N., and Felber, B. K. (2006) *Retrovirology* **3**, 6–14
- Smulevitch, S., Michalowski, D., Zolotukhin, A. S., Schneider, R., Bear, J., Roth, P., Pavlakis, G. N., and Felber, B. K. (2005) *J. Virol.* **79**, 2356–2365
- Taberner, C., Zolotukhin, A. S., Valentin, A., Pavlakis, G. N., and Felber, B. K. (1996) *J. Virol.* **70**, 5998–6011
- Guzik, B. W., Levesque, L., Prasad, S., Bor, Y. C., Black, B. E., Paschal, B. M., Rekosh, D., and Hammarshjöld, M. L. (2001) *Mol. Cell. Biol.* **21**, 2545–2554
- Braun, I. C., Herold, A., Rode, M., Conti, E., and Izaurralde, E. (2001) *J. Biol. Chem.* **276**, 20536–20543
- Zhou, Z., Luo, M. J., Straesser, K., Katahira, J., Hurt, E., and Reed, R. (2000) *Nature* **407**, 401–405
- Zenklusen, D., Vinciguerra, P., Strahm, Y., and Stutz, F. (2001) *Mol. Cell. Biol.* **21**, 4219–4232
- Stutz, F., Bachi, A., Doerks, T., Braun, I. C., Séraphin, B., Wilm, M., Bork, P., and Izaurralde, E. (2000) *RNA* **6**, 638–650
- Hautbergue, G. M., Hung, M. L., Golovanov, A. P., Lian, L. Y., and Wilson, S. A. (2008) *Proc. Natl. Acad. Sci. U.S.A.* **105**, 5154–5159
- Golovanov, A. P., Hautbergue, G. M., Tintaru, A. M., Lian, L. Y., and Wilson, S. A. (2006) *RNA* **12**, 1933–1948
- Rodrigues, J. P., Rode, M., Gatfield, D., Blencowe, B. J., Carmo-Fonseca, M., and Izaurralde, E. (2001) *Proc. Natl. Acad. Sci. U.S.A.* **98**, 1030–1035
- Zhou, Z., Licklider, L. J., Gygi, S. P., and Reed, R. (2002) *Nature* **419**, 182–185
- Katahira, J., Strässer, K., Podtelejnikov, A., Mann, M., Jung, J. U., and Hurt, E. (1999) *EMBO J.* **18**, 2593–2609
- Bachi, A., Braun, I. C., Rodrigues, J. P., Panté, N., Ribbeck, K., von Kobbe, C., Kutay, U., Wilm, M., Görlich, D., Carmo-Fonseca, M., and Izaurralde, E. (2000) *RNA* **6**, 136–158
- Kuznetsov, V. (2003) in *Computational and Statistical Approaches to Genomics*, pp. 125–171, Springer-Verlag New York Inc., New York

OTT3 and RBM15 Function

48. Hansen, A., Chen, Y., Inman, J. M., Phan, Q. N., Qi, Z. Q., Xiang, C. C., Palkovits, M., Cherman, N., Kuznetsov, S. A., Robey, P. G., Mezey, E., and Brownstein, M. J. (2007) *Nat. Methods* **4**, 35–37
49. Tan, W., Zolotukhin, A. S., Tretyakova, I., Bear, J., Lindtner, S., Smulevitch, S. V., and Felber, B. K. (2005) *Nucleic Acids Res.* **33**, 3855–3865
50. Zhang, M., Wang, Q., and Huang, Y. (2007) *Proc. Natl. Acad. Sci. U.S.A.* **104**, 10057–10062
51. Takano, K., Miki, T., Katahira, J., and Yoneda, Y. (2007) *Nucleic Acids Res.* **35**, 2513–2521
52. Saito, K., Fujiwara, T., Katahira, J., Inoue, K., and Sakamoto, H. (2004) *Biochem. Biophys. Res. Commun.* **321**, 291–297
53. Kuersten, S., Segal, S. P., Verheyden, J., LaMartina, S. M., and Goodwin, E. B. (2004) *Mol. Cell* **14**, 599–610
54. Jun, L., Frints, S., Duhamel, H., Herold, A., Abad-Rodrigues, J., Dotti, C., Izaurrealde, E., Marynen, P., and Froyen, G. (2001) *Curr. Biol.* **11**, 1381–1391
55. Herold, A., Suyama, M., Rodrigues, J. P., Braun, I. C., Kutay, U., Carmo-Fonseca, M., Bork, P., and Izaurrealde, E. (2000) *Mol. Cell. Biol.* **20**, 8996–9008
56. Lai, D., Sakkas, D., and Huang, Y. (2006) *RNA* **12**, 1446–1449